J. Earth Syst. Sci. (2020)129 70
https://doi.org/10.1007/s12040-019-1338-8

Latent heat flux variation during the warming phase of intraseasonal oscillations over northern Bay of Bengal

Simi Mathew[1,*], G Latha[2] and R Venkatesan[2]

[1]*Centre for Water Resources, Anna University, Guindy Campus, Chennai 600 025, India.*
[2]*National Institute of Ocean Technology, Pallikaranai P.O, Chennai 600 100, India.*
**Corresponding author. e-mail: simikennady@gmail.com*

MS received 1 August 2019; revised 8 November 2019; accepted 13 November 2019

The sensitivity of latent heat flux to the warming phase of intra-seasonal oscillation in the Bay of Bengal is studied with the help of in-situ data. This was analyzed from 2012 to 2015 with the help of data obtained from moored buoys deployed in the northern Bay of Bengal. The annual secondary peaks in sea surface temperature is observed in the northern Bay of Bengal associated with the warming phase of the intra-seasonal oscillation during southwest monsoon season, with net heat flux dominantly governing the mixed layer temperature. An increase in the release of latent heat flux from the northern bay is observed with the warming phase of intra-seasonal oscillation, which again leads to cooling of sea surface temperature. Higher latent heat flux release associated with the intra-seasonal warming phase during southwest monsoon season has intrigued us to study the sensitivity of latent heat flux with sea surface temperature. The sensitivity of gradient in saturation specific humidity is comparatively higher than the sensitivity of wind speed to sea surface temperature variations during southwest monsoon season. The gradient in sea–air saturation specific humidity is largely driven by saturation specific humidity of air (Q_a) during both the seasons. However, the correlation of gradient in saturation specific humidity with surface saturation specific humidity is higher during southwest monsoon season compared to northeast monsoon season. Thus, the warming phase of sea surface temperature associated with intra-seasonal oscillation during southwest monsoon season always lead to an increase in latent heat flux release, favoured by high sensitivity of surface saturation specific humidity to variations in sea surface temperature.

Keywords. Intra-seasonal oscillation; latent heat flux; NEM; sea surface temperature; SWM.

1. Introduction

The sea surface temperature (SST) of Bay of Bengal (BoB) is positively correlated with the Indian summer monsoon with intra-seasonal oscillation (ISO) in SST, reflected as active and break phase of monsoon (Sengupta and Ravichandran 2001). The active break cycle is the result of strong ocean-atmosphere coupled phenomenon; with SST, convection, low level jet and net heat flux at the ocean surface playing the major roles (Joseph and Sabin 2008). During active phases, there is strengthening of the monsoon jet, increased deep atmospheric convection over eastern Arabian Sea and BoB (Goswami and Ajayamohan 2001). The intra-seasonal SST changes are mainly driven by net surface heat flux and its northward propagation is strongly coupled with the underlying SST (Sengupta *et al.* 2001). The maximum convective perturbation propagates northward, from 5° to

Published online: 15 February 2020

about 20°N in 20 days (Goswami 2005). Eastern Indian Ocean, east of 65°E had the strongest surface flux perturbations of around 20–30 Wm^{-2} due to the northward movement of the active-break cycle, with negative heat flux perturbations associated with increased convection and surface wind during the active phase (Vialard *et al.* 2012). Heat fluxes are always the dominant processes in the northern BoB region, with wind stress occasionally contribute up to 40% of the SST variations. The strong quadrature relationship (∼90° phase lag) between precipitation and SST is certainly a feature of the northward propagating monsoon ISO (Jayakumar *et al.* 2017). The intra-seasonal SST signal in the northern Indian Ocean has the strongest association with the active/break index and it is a useful index for the prediction of active and break spells of south Asian summer monsoon with a lead of at least 10 days (Fu *et al.* 2003). Lead/lag correlation between SST and precipitation over both monsoon basins have shown that the precipitation increases throughout the observed SSTs over Arabian Sea and BoB (26–31°C) (Roxy 2014). In-situ data obtained from this location continuously for four consecutive southwest monsoon (SWM) seasons were analysed to understand the lead-lag correlation between SST and latent heat flux (LHF), especially during the ISO warming phase. Enhanced convective activity associated with the active phase of monsoon ISO leads to cooling of mixed layer temperature of maximum amplitude in the central and northern BoB (Girishkumar *et al.* 2017). The increased release of LHF observed in the northern BoB associated with ISO warming phase can be either due to large variability in gradient in sea–air saturation-specific humidity or higher variability of wind speed with SST. The sub-seasonal variability in sea–air saturation specific humidity gradient contributes equally or more to latent heat flux variability when compared to the wind speed during both the seasons. It is also known that the variability in sea–air saturation specific humidity gradient showed stronger seasonal dependence with increasing distance from the equator with lowest values observed during the summer monsoon and it closely followed SST, when SST is greater than 28°C (Bhat 2003). Thus, the warming phase of ISO supports large release of LHF into the atmosphere. However, BoB and northern Arabian Sea behaves in an exceptional way in the temperature range of 25–28°C, for the sensitivity of LHF to SST (Kumar *et al.* 2017), as the temperature increases in these basins, air temperature increases faster than SST and favours a decrease in surface air humidity difference resulting in a decrease of LHF. During winter the latent heat loss was maximum accompanied by the drier air of the season compared to summer monsoon associated with higher humidity (Weller *et al.* 2016). An extensive study on the sensitivity of LHF to SST was carried out with the continuous data obtained from the moored buoys in the northern BoB. We have looked into the sensitivity of LHF to SST during both the seasons by analyzing the sensitivity of gradient in saturation specific humidity with SST and sensitivity of wind speed with SST, separately. The correlation of sea–air saturation-specific humidity gradient with SST during both the seasons was studied and their correlation with surface saturation specific humidity and atmospheric saturation specific humidity were analyzed separately. The LHF response to increase in SST above 29°C associated with the warming phase of ISO events during SWM season is analyzed by looking into such cases from 2012 to 2015.

2. Data and methods

The Ministry of Earth Sciences, Government of India has initiated the National Data Buoy Programme (NDBP) in 1997 under National Institute of Ocean Technology (NIOT), Chennai to make real time surface meteorological and near-surface oceanographic measurements (Premkumar *et al.* 1999). A continuous record of surface meteorological as well as oceanographic data such as surface temperature, salinity and current data were made available through this initiative. However, measurements of temperature, salinity and currents from sub-surface depths was initiated later with the deployment of Ocean Moored Network for the northern Indian Ocean named as OMNI buoys at six specific locations in the BoB during June, 2011 as shown in figure 1. The accuracy and resolution of all the sensors used in the OMNI buoys are of World Meteorological Organization (WMO) standards and the sensors are send back to the manufacturer once in a year, for calibration (Venkatesan *et al.* 2013). The ISO warming phase are identified from the surface data obtained from the moored buoys named as BD08 and BD09 deployed at 89.7°E/18.2°N and 89.7°E/17.8°N, respectively in the northern BoB, during SWM season (July–September). The heat flux components such

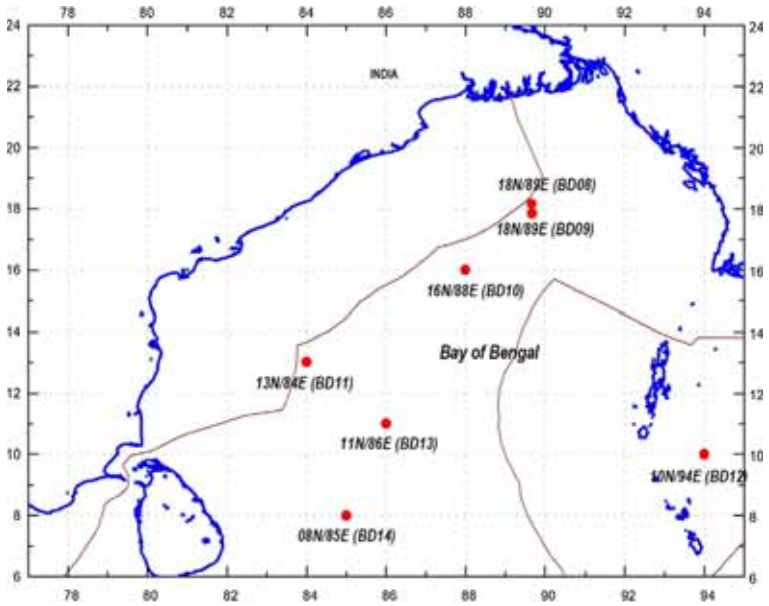

Figure 1. The location of the OMNI buoys in the BoB marked along with the exclusive economic zone.

as latent heat flux (Q_{lhf}) and sensible heat flux (Q_{shf}) were estimated with the help of Coupled Ocean Atmosphere Response Experiment (COARE-3.5) algorithm developed by Fairall *et al.* (2003). LHF is computed traditionally using the bulk formula

$$\text{LHF} = \rho L_v C_h W_s \Delta q, \tag{1}$$

where ρ is the air density (kg m^{-3}), L_v is the latent heat of vapourization (2.44×10^6 J kg^{-1}), C_h is the transfer coefficient (1.3×10^{-3}), W_s is the wind speed at 10 m above the sea surface and Δq is the difference in saturation specific humidity of sea surface (Q_s) and air (Q_a). The relative contribution of wind speed and saturation specific humidity gradient to the LHF was determined by differentiating equation (1) with respect to SST (Kumar *et al.* 2017) and is expressed as follows.

$$\underbrace{\frac{\text{dLHF}}{\text{dSST}}}_{\text{c}} = \underbrace{\rho L_v C_h \left[\frac{dW_S}{dSST}\Delta q\right]}_{\text{a}} + \underbrace{\rho L_v C_h \left[\frac{d\Delta q}{dSST} W_S\right]}_{\text{b}} \tag{2}$$

Equation (2) has two components, the dynamic component, i.e., the first term (a) and the thermodynamic component, i.e., the second term (b). The percentage of wind speed variation with SST to the total variation of LHF with SST and percentage of saturation specific humidity gradient with SST to the total variation of LHF with SST is measured for SWM season and NEM season by computing the absolute value of a/c×100 and b/c×100, respectively.

3. ISO warming phase of the northern BoB

The ISO of large amplitude is observed in the northwestern part of BoB due to the large influx of river discharges into the bay during summer monsoon (Vinayachandran *et al.* 2012). The ISO in SST with active phase associated with high wind speed and deep atmospheric convection followed by break phase with low wind speed and weak atmospheric convection was observed during summer monsoon (Sengupta *et al.* 2001). The SST anomaly based on Advanced Microwave Scanning Radiometer for EOS (AMSR-E) for the warming phase and cold phase of an active/break cycle of ISO during 2013 is plotted in figure 2. In-situ data obtained from the moored buoys deployed in the northern BoB, monitored the ISO in SST during SWM season (July to September) from 2012 to 2015. The dates corresponding to the negative and positive anomalous SST during an active/break phase of ISO during 2013 were 26th August and 13th September, respectively. The northern half of the BoB is anomalously warm during the warming phase of ISO and there is a large north–south gradient in SST as shown in figure 2(a). However, the north–south gradient in SST completely collapses during the cold phase (figure 2b). Summer monsoon warming is characterized by intense

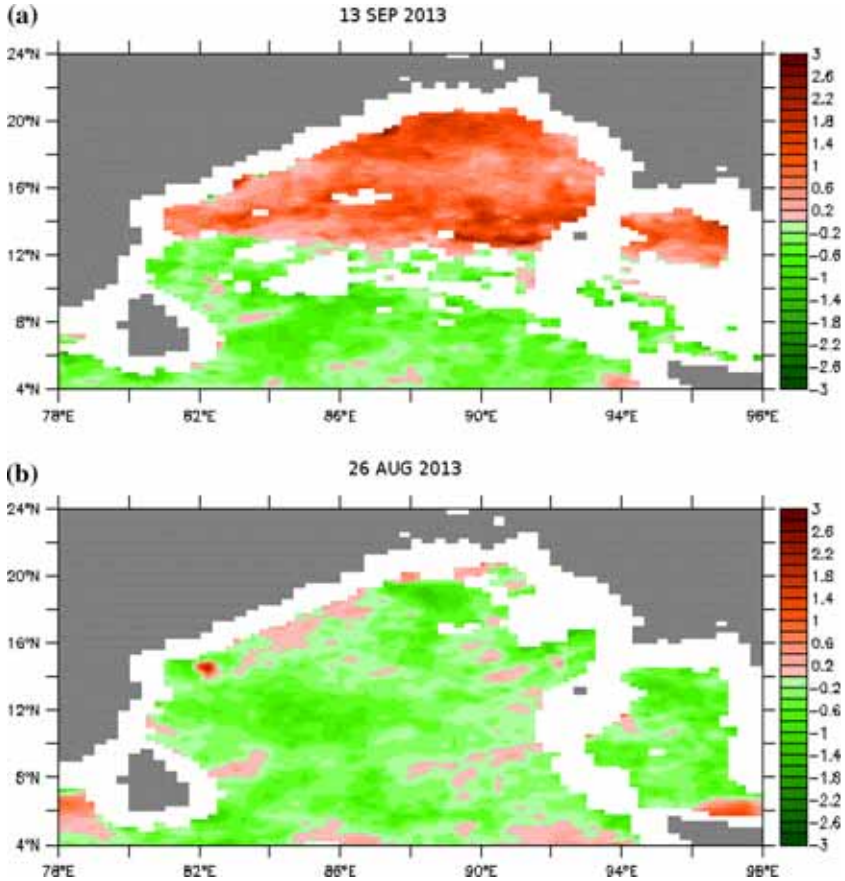

Figure 2. (**a**) The SST anomaly during the warming phase (13th September) and **(b)** cooling phase of ISO (26th August) during 2013.

solar heating confined to the shallow MLD, with highly stratified waters further restrains cooling by turbulent mixing (Shenoi *et al.* 2002). Several earlier studies have reported dominant role of net heat flux in the warming phase of the mixed layer during SWM season (Rao and Sivakumar 2003; Parampil *et al.* 2010; Thangaprakash *et. al.* 2016). The Fast Fourier transform (FFT) of SST data recorded during June–February from 2012 to 2015, clearly supported the presence of ISO with periodicity of 20–40 days (figure 3). The SST data recorded during 2013 had dominant peaks at 18, 27 and 41 days as shown in figure 3(b). The SST peaked above 29°C, with maximum SST of 29.2°, 29.3° and 29.9°C recorded during mid of July, August and September, respectively, as shown in figure 4(b). While in 2012, the peak periods of ISO were recorded at 22, 26, 38 and 53 days as shown in figure 3(a). The SST peaked during mid of July followed by peak in SST recorded during end of August and September as shown in figure 4(a). Due to the unavailability of data from surface sensors, we have looked into the temperature data collected by the CT sensor at 10 m depth, with recorded temperature values of 29.4°, 28.8° and 29.5°C, respectively. The bulk surface temperature recorded by Accoustic Doppler Current Profiler (ADCP) at 7 m depth also recorded similar ISO warming episodes. In 2014, peak frequencies were recorded at 20, 40 and 61 days (figure 3c). The ISO warming episodes with SST crossing 29°C were recorded during mid of June, July and end of August and first week of October as shown in figure 4(c). The ISO with similar periodicity was recorded during 2015, with SST crossing 29°C during mid of July, August and first week of September and October as shown in figure 4(d). The peak periods of ISO were recorded at 18, 25, 35 and 61 days as shown in figure 3(d). However, there were signals of higher frequencies in the SST data, especially during 2012 and 2015. In order to remove the higher frequencies, a 10-day low pass filter was applied on the SST data. We have further analyzed the impact of warming phase of ISO on the LHF released from the ocean. The sensitivity of LHF to the ISO warming phase is addressed by studying the sensitivity of wind speed and sensitivity of

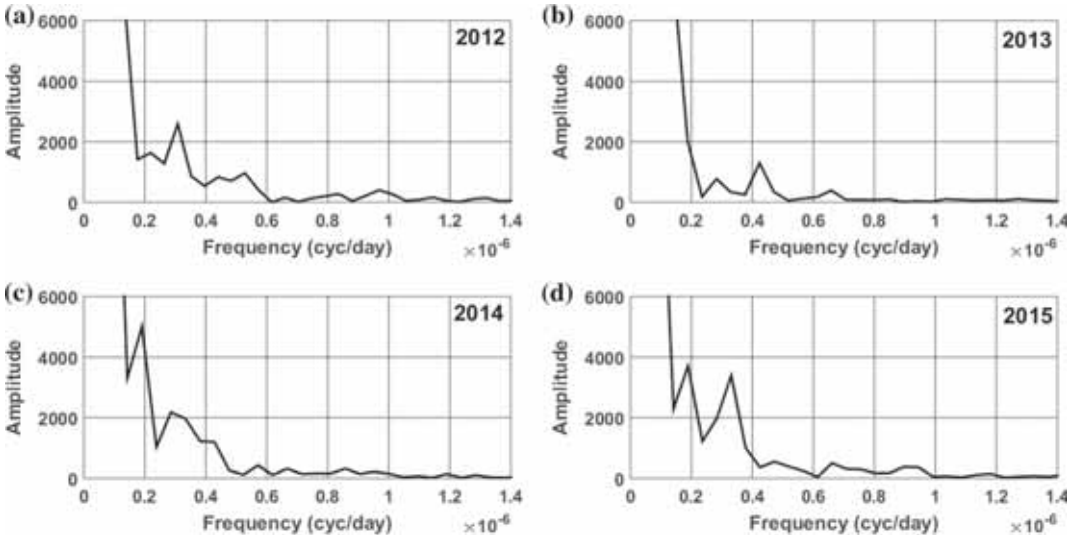

Figure 3. The dominant frequencies of around 20, 40 and 60 days observed in the SST data recorded by BD09 during **(a)** 2012, **(b)** 2013, **(c)** 2014 and **(d)** 2015.

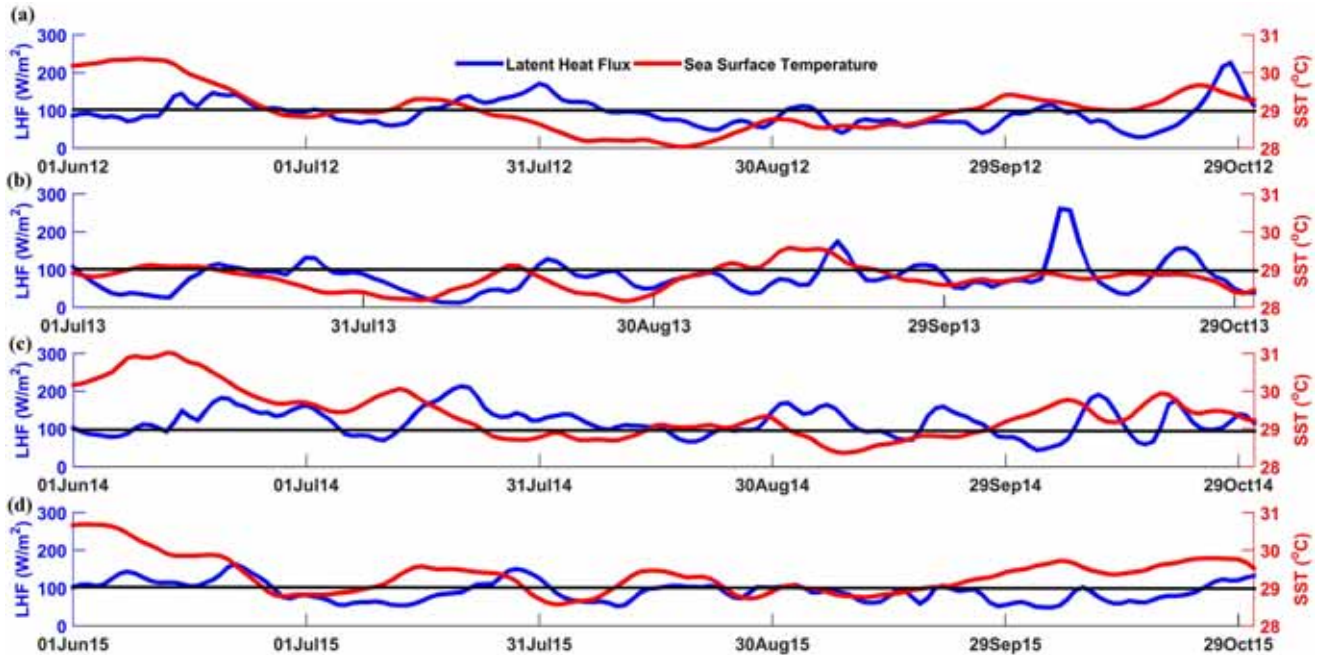

Figure 4. The SST plotted against Latent Heat Flux from July to October for **(a)** 2012, **(b)** 2013, **(c)** 2014 and **(d)** 2015.

sea–air saturation-specific humidity gradient with respect to SST, separately.

4. Intense release of latent heat flux associated with the ISO warming phase

Whether the warming phase of ISO is associated with large release of LHF? LHF computed from 2012 to 2015, using surface data obtained from the buoys in the northern BoB showed secondary peaks during SWM season. These peaks were associated with the warming phase of ISO as they both co-occurred with a lag of few days as shown in figure 4. The bulk release of LHF during mid-September of 2013, measured to 235 W/m^2 and LHF release of the order of 135 and 162 W/m^2 during mid of July and August were associated with ISO warming phase. There is also an observed intensification in LHF release associated with cyclonic storms in the BoB. An intensification of LHF of the order of 385 W/m^2 was recorded during

11th October of 2013, associated with the Phailin cyclone. However, this increase in LHF is associated with the high wind speed and occurs with no phase lag with SST as shown in figure 4(b). During 2012, the ISO warming phase initiated an increase in the release of LHF during mid of July and peaked to 190 W/m^2 towards end of July. There were two more peaks in LHF associated with the warming phase during last week of August and September as shown in figure 4(a). During 2014, warming was more pronounced during mid of July, with an observed maximum release of LHF of 218 W/m^2, recorded on 19th of July. Another warming phase initiated during late September with a measured LHF release of 234 W/m^2 on 9th of October. It was also associated with the passage of cyclonic storm, Hudhud. Similarly, the LHF response to ISO warming phase during 2015 also showed a lead lag correlation, with SST leading LHF by few days (figure 4d). The peak in SST observed during 18 June–15 July was followed by intensification of LHF recorded during 21 June–26 July. Similar intensification of LHF was observed during mid and last week of August and during first week of October followed by the warming phase of ISO. A 10-day low pass filter is applied on both SST and LHF data to remove the higher frequencies and a lead lag correlation of LHF against SST was carried out for all the 4 years. The maximum correlation was obtained at a lag of 5 days during 2013 and 2015 (figure 5). Maximum correlation occurred at a lag of 15 days during 2012 and 8 days during 2014 as shown in figure 5. Thus the warming phase of ISO always leads to an intense release of LHF over northern BoB with a lag of 5–15 days. Latitude time lag of SST, low level atmospheric parameters and precipitation based on satellite observations have shown that the northward propagating dynamical surface convergence and SST anomalies tend to form a favourable condition for enhanced convective activity over AS and BoB (Roxy and Tanimoto 2007). A similar study based on global seasonal forecast system version 5 (GloSea5), an initialized coupled model also depicted the ∼90 phase relationship between precipitation and SST, with warm SST leading the positive phase of the convective anomaly over the head BoB (Jayakumar *et al.* 2017). In this study, in-situ data were used to compute the lead lag correlation of SST and LHF during SWM season for four consecutive years.

An increase in SST favours an increase in sea–air saturation specific humidity gradient (Q_s–Q_a) due to the proportionality of surface saturation specific humidity (Q_s) with SST in the BoB (Weller *et al.* 2016). The higher correlation of the Q_s–Q_a term with SST during SWM season compared to NEM season supports the intensification of LHF with increase in SST during SWM season. The correlation seems to be higher during SWM season with a magnitude of 0.56 during SWM season, compared to 0.14 during NEM season as shown in the top panel of figure 6. Thus Q_s–Q_a term responds quickly to SST variations during SWM season. However, the negative correlation of Q_s–Q_a with Q_a, during both the seasons are very high and comparable, with correlation coefficient of –0.84 during SWM season and –0.72 during NEM season as shown in lower panel of figure 6. The inverse effect of saturated specific humidity of air (Q_a) on

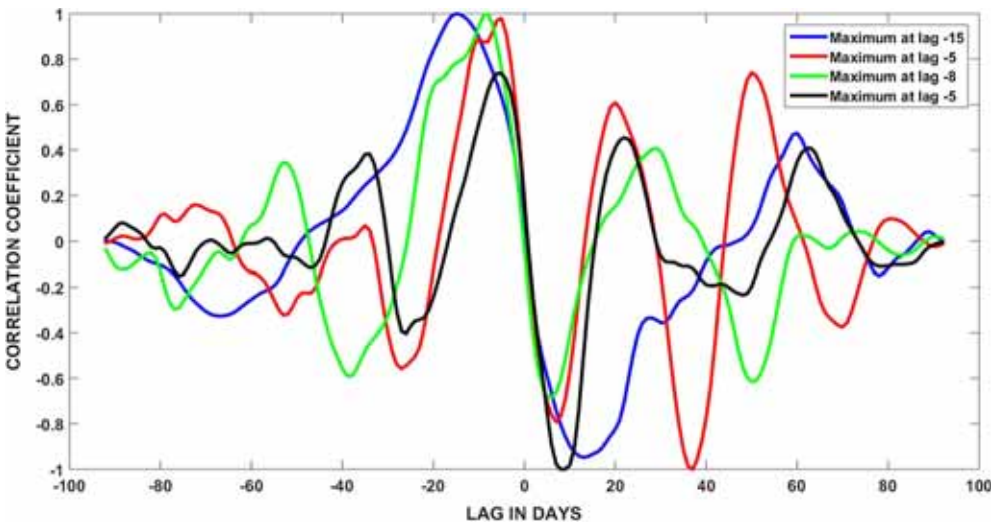

Figure 5. The lead lag correlation of SST vs LHF during SWM season for the years **(a)** 2012, **(b)** 2013, **(c)** 2014 and **(d)** 2015.

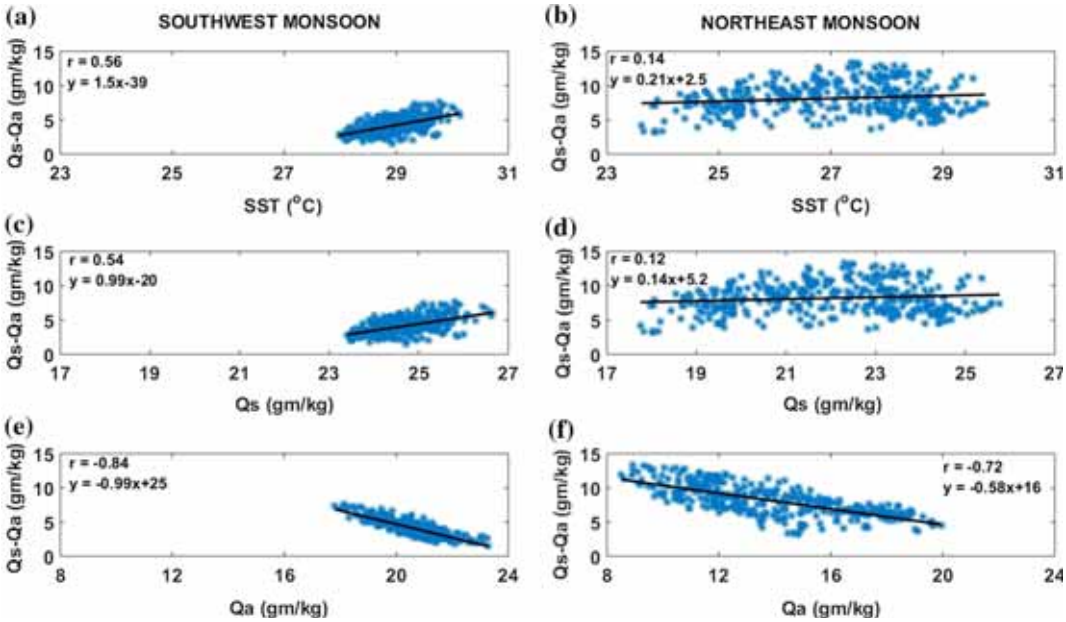

Figure 6. The correlation of gradient of saturation specific humidity against SST (**a, b**), surface saturation specific humidity (Q_s) (**c, d**) and air saturation specific humidity (Q_a) (**e, f**), during SWM and NEM season, respectively.

LHF has been reported during summer monsoon and winter monsoon season over southern BoB (Rahman and Ravichandran 2013). The correlation of Q_s–Q_a to Q_s term also shows higher correlation during SWM season even though the range of SST, Q_s–Q_a, Q_s and Q_a is very small compared to NEM season. The Q_s–Q_a term increases with SST in both AS and BoB in most of the seasons, except when SST is in the range 25–28°C (Praveen Kumar *et al.* 2017). Thus, the LHF is more sensitive to SST variability during SWM season.

5. Sensitivity of LHF to ISO warming phase

An analysis on the sensitivity of LHF to SST variations was carried out by quantifying the contributions of dynamic component (wind speed) and thermodynamic component (sea–air saturation-specific humidity gradient), separately as explained in section 2. The absolute percentage of dynamic and thermodynamic component to the total derivative of LHF to SST is computed and averaged over the SWM and NEM season of 2013, 2014 and 2015 (figure 7). The sensitivity of LHF to SST variations was mostly driven by dynamic component during both seasons, (i.e., the first term in equation 2) with an average of 63 and 68 percentages during SWM and NEM season, respectively as shown in figure 7. However, the thermodynamic component, i.e., the second term in equation (2) contributed equally or more to the total variability compared to dynamic component during SWM season. The average percentage of the thermodynamic component was around 37 and 32 during the 91 days of SWM and NEM season, respectively (figure 7). The number of occurrences of thermodynamic component greater than 50% doubled during the SWM season compared to NEM season. Thus the sensitivity of LHF to SST is large during SWM season due to the added variability of gradient in saturation specific humidity with SST. The dynamic component opposes increase of LHF at warmer SST and thermodynamic component favours an increase in LHF when SST is greater than 28°C (Praveen Kumar *et al.* 2017). Similar characteristics of LHF are observed in Pacific Ocean, wherein the LHF decreases with increase in SST due to sharp decrease in wind speed at high SST (Zhang and McPhaden 1995). The percentage contribution of the dynamic component reduced during SWM season compared to NEM season with the number of occurrences of greater than 50% reduces from 80 to 68. Thus at higher SST during SWM season the thermodynamic component contribution to the total LHF variability is more significant. A decrease in SST followed by the intense release of LHF is observed in all the 4 years as shown in figure 4. It is in line with the earlier heat budget analysis study which established the role of net heat flux in controlling the mixed layer temperature of northern BoB during SWM season, with LHF and shortwave radiation playing the major roles (Parampil *et al.* 2016).

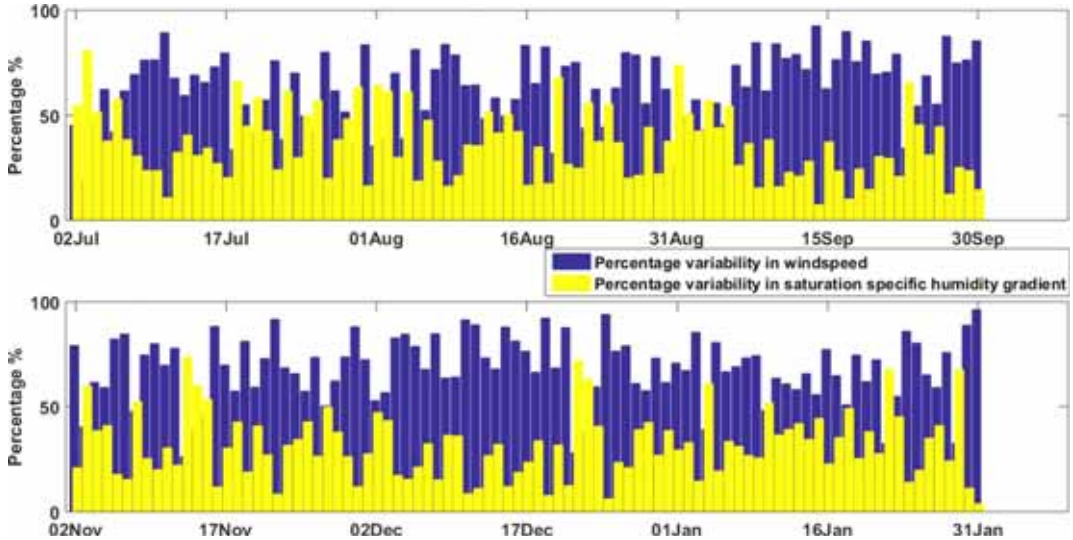

Figure 7. The percentage fraction of wind speed variability with SST (blue bars) and percentage fraction of saturation specific humidity gradient with SST (yellow bars) to the total variability of LHF to SST during SWM season (top panel) and NEM season (bottom panel).

6. Conclusions

Intra-seasonal oscillation in warming of the order of 1.5–2°C is observed in the northern BoB during SWM season, with a periodicity of 20–40 days. The intra-seasonal warming phases are associated with an increased release of LHF with a lag of 5–15 days. The LHF is highly sensitive to SST variations during SWM season due to the larger contribution of the thermo-dynamic component to the total variability. The correlation of saturation specific humidity gradient (Q_s–Q_a) to SST and Q_s is higher during SWM season compared to NEM season. However, the correlation of saturation specific humidity gradient (Q_s–Q_a) to Q_a remains the same during both the seasons. Thus a similar variation in SST will have larger impact on the thermodynamic component during SWM season compared to NEM season. A cooling of SST with the intense release of LHF observed during all the years highlighted the role of LHF as a major component of net heat flux term in controlling the mixed layer temperature. Thus, the ISO warming phase in the northern Bay of Bengal during SWM season initiates a positive feedback for moisture supply with larger release of LHF.

Acknowledgements

Our sincere thanks are due to Dr Robert Weller (WHOI, USA), for guiding us through the analysis. We sincerely thank the technical staff of Ocean Observation Systems of NIOT, for the continuous efforts for maintaining the moorings at sea. Thanks are due to MoES for all the support provided through various training programs.

References

Bhat G S 2003 Measurement of air sea fluxes over the Indian Ocean and the Bay of Bengal; *J. Clim.* **16(4)** 767–775.

Fairall C W, Bradley E F, Hare J E, Grachev A A and Edson J B 2003 Bulk parameterization on air–sea fluxes: updates and verification for the COARE algorithm; *J. Clim.* **16** 571–591.

Fu X, Wang B, Li T and McCreary J P 2003 Coupling between northward propagating intra-seasonal oscillations and sea surface temperature in the Indian Ocean; *J. Atmos. Sci.* **60(15)** 1733–1783.

Girishkumar M S, Joseph J, Thangaprakash V P, Pottapinjara V and McPhaden M J 2017 Mixed layer temperature budget for the northward propagating summer monsoon intra-seasonal oscillation (MISO) in the central Bay of Bengal; *J. Geophys. Res.* **122(11)** 8841–8854.

Goswami B N 2005 Intraseasonal variability in the atmosphere–ocean climate system (eds) Lau W K M and Waliser D E, Berlin, Praxis-Springer, South Asian Monsoon, pp. 19–55.

Goswami B N and Ajayamohan R S 2001 Intra-seasonal oscillations and interannual variability of the Indian summer monsoon; *J. Clim.* **14** 1180–1198.

Jayakumar A, Turner A, Johnson S, Rajagopal E, Mohandas S and Mitra A 2017 Boreal summer sub-seasonal variability of the South Asian monsoon in the met office GloSea5 initialized coupled model; *Clim. Dyn.* **49(5–6)** 2035–2059.

Joseph P V and Sabin T P 2008 An ocean–atmosphere interaction mechanism for the active break cycle of the Asian summer monsoon; *Clim. Dyn.* **30(6)** 553–566.

Kumar B P, Cronin M F, Joseph S, Ravichandran M and Suresh Kumar N 2017 Latent heat flux sensitivity to sea

surface temperature: regional perspectives; *J. Clim.* **30(1)** 129–143.

Parampil S R, Anita G, Ravichandran M and Sengupta D 2010 Intraseasonal response of mixed layer temperature and salinity in the Bay of Bengal to heat and freshwater flux; *J. Geophys. Res.* https://doi.org/10.1029/2009jc005790.

Parampil S R, Bharathraj G N, Harrison M and Sengupta D 2016 Observed sub-seasonal variability of heat flux and SST response of the tropical Indian Ocean; *J. Geophys. Res.* **121(10**) 7290–7307.

Premkumar K, Ravichandran M, Kalsi S R, Sengupta D and Gadgil S 1999 First results from new observational system over the Indian Seas; *Curr. Sci.* **78(3)** 323–330.

Rahman H and Ravichandran M 2013 Evaluation of near-surface air temperature and specific humidity from hybrid global products and their impact on latent heat flux in the Northern Indian Ocean; *J. Geophys. Res.* **118(2)** 1034–1047.

Rao R R and Sivakumar R 2003 Seasonal variability of sea surface salinity and salt budget of the mixed layer of the northern Indian ocean; *J. Geophys. Res.* **108(C1)** 3009, https://doi.org/10.1029/2001jc000907.

Roxy M K 2014 Sensitivity of precipitation to sea surface temperature over the tropical summer monsoon region and its quantification; *Clim. Dyn.* **43(5–6)** 1159–1169.

Roxy M K and Tanimoto Y 2007 Role of SST over the Indian Ocean in influencing the intra-seasonal variability of the Indian summer monsoon; *J. Meteor. Soc. Japan* **85(3)** 349–358.

Sengupta D and Ravichandran M 2001 Oscillations of Bay of Bengal sea surface temperature during the 1998 summer monsoon; *Geophys. Res. Lett.* **28(10)** 2033–2036.

Sengupta D, Goswami B N and Senan R 2001 Coherent intraseasonal oscillations of ocean and atmosphere during the Asian summer mnsoon; *Geophys. Res. Lett.* **28(21)** 4127–4130.

Shenoi S S C, Shankar D and Shetye S R 2002 Differences in heat budgets of the near-surface Arabian Sea and Bay of Bengal: implications for the summer monsoon; *J. Geophys. Res.* **107(C6)** 1–14.

Thangaprakash V P, Girishkumar M S, Suprit K, Suresh Kumar N, Chaudhuri D, Dinesh K, Kumar A, Shivaprasad S, Ravichandran M, Farrar J T, Sundar R and Weller R A 2016 What controls seasonal evolution of sea surface temperature in the Bay of Bengal? Mixed layer heat budget analysis using moored buoy observations along 90°E; *Oceanography* **29(2)** 202–213.

Venkatesan R, Shamji V R, Latha G, Mathew S, Rao R R, Muthiah M A and Atmanand M A 2013 In-situ ocean observation time series measurements from OMNI buoy network in the Bay of Bengal; *Curr. Sci.* **104(9)** 1166–1177.

Vialard J, Jayakumar A, Gnanaseelan C, Lengaigne M, Sengupta D and Goswami B N 2012 Processes of 30–90 days of sea surface temperature variability in the northern Indian Ocean during boreal summer; *Clim. Dyn.* **38(9–10)** 1901–1916.

Vinaychandran P N, Neema C P, Mathew S and Remya R 2012 Mechanisms of summer intra-seasonal sea surface temperature oscillations in the Bay of Bengal; *Geophys. Res. Lett.* **117(C01005)** 1–15.

Weller R A, Farrar T J, Buckley J, Mathew S, Venkatesan R, Sree Lekha J, Chaudhari D, Suresh Kumar N and Praveen Kumar B 2016 Air–sea interaction in the Bay of Bengal; *Oceanography* **29 (2)** 28–37.

Zhang G J and McPhaden M J 1995 The relationship between sea surface temperature and latent heat flux in the equatorial Pacific; *J. Clim.* **8(3)** 589–605.

Corresponding editor: C. Gnanaseelan